Structural, electrical and optical properties of aluminum doped zinc oxide films prepared by radio frequency magnetron sputtering

Kun Ho Kim[a)]
Department of Physics and the Research Institute of Natural Science, Gyeongsang National University, Chinju 660-701, Korea

Ki Cheol Park and Dae Young Ma
Department of Electronic Materials Engineering and Research Center for Aircraft Parts Technology, Gyeongsang National University, Chinju 660-701, Korea

(Received 15 October 1996; accepted for publication 17 March 1997)

Aluminum doped zinc oxide (AZO) films are prepared by rf magnetron sputtering on glass or Si substrates using specifically designed ZnO targets containing different amount of Al_2O_3 powder as the Al doping source. The structural, electrical, and optical properties of the AZO films are investigated in terms of the preparation conditions, such as the Al_2O_3 content in the target, rf power, substrate temperature and working pressure. The crystal structure of the AZO films is hexagonal wurtzite. The orientation, regardless of the Al content, is along the *c* axis perpendicular to the substrate. The doping concentration in the film is 1.9 at. % for 1 wt % Al_2O_3 target, 4.0 at. % for 3 wt % Al_2O_3 target, and 6.2 at. % for 5 wt % Al_2O_3 target. The resistivity of the AZO film prepared with the 3 wt % Al_2O_3 target is $\sim 4.7\times 10^{-4}$ Ω cm, and depends mainly on the carrier concentration. The optical transmittance of a 1500-Å-thick film at 550 nm is ~90%. The optical band gap depends on the Al doping level and on the microstructure of the films, and is in the range of 3.46–3.54 eV. The optical band gap widening is proportional to the one-third power of the carrier concentration. © *1997 American Institute of Physics.* [S0021-8979(97)04312-0]

I. INTRODUCTION

Transparent conductive films such as Sn-doped In_2O_3 (ITO), SnO_2 (NESA) and ZnO have been widely studied for their practical applications as transparent electrodes, window materials in display, solar cells, and various optoelectronic devices.[1–4] ZnO films are very attractive due to their ease in doping Si,[5] Ga,[6,7] Al, and so on. Al-doped ZnO (AZO) transparent conductive film has high transmittance in the visible region, low resistivity, and the optical band gap can be controlled by the Al doping level.[3,4,8–13] AZO film can be prepared by various methods, e.g., vacuum evaporation, chemical vapor deposition, spray pyrolysis, and sputter deposition. Sputtering is the most widely used technique for preparing AZO films.[9,12,14,15] For AZO film growth, two types of sputtering are commonly applicable according to the Al doping method. One is co-sputtering of the Al target and ZnO targets,[14] the other is the conventional sputtering of a ZnO+ Al_2O_3 target.[3,9,12]

Studies of AZO films prepared by sputter deposition have shown that the AZO films are strongly oriented perpendicular to the substrate surface (*c*-axis orientation), have a polycrystalline hexagonal wurtzite structure[8,10,11,14] and have properties of transparent electrodes comparable to ITO or NESA with resistivities as low as 10^{-4} Ω cm and optical transmittance of ~90% in the visible region. They cost less in raw material, and have good thermal stability; moreover, they are more stable in a hydrogen plasma ambient than ITO or NESA,[3,11,16] and thus, many studies have been concentrated on replacing ITO or NESA with AZ0 films.[4–6]

The structural, optical, and electrical properties of AZO films are influenced by deposition parameters such as the Al_2O_3 content in the target, substrate temperature, ambient gas and pressure, and rf power.[8,11,12] It is, therefore, of great value to study the effects of the deposition parameters in order to obtain AZO films with optimum properties.

In this article we report on the physical properties of AZO films prepared by rf magnetron sputter deposition using a 4 inch target that was made from high purity ZnO powder containing different amounts of Al_2O_3 powder as the Al doping source. The chemical composition, the doping level, and the structural properties were investigated according to various deposition parameters. The crystallinity, crystal structure, and growth orientation were examined by x-ray diffraction (XRD), and the surface morphology was studied by scanning electron microscopy (SEM). The chemical compositions were investigated by energy dispersive (EDS) x-ray analysis and 2 MeV $^4He^{++}$ ion backscattering spectrometry (RBS). The electrical properties were investigated by the Hall coefficient and by resistivity measurements. The optical properties were studied by measuring the transmittance in the visible region and by analyzing the relationship between the widening of band gap with carrier concentration.

II. EXPERIMENT

The sputtering targets used in the experiment were ones that were specifically designed using high purity ZnO (99.99%) and Al_2O_3 (99.99%) powders. Four different targets with different weight percent (wt %) Al_2O_3 were prepared: (1) pure ZnO, (2) 1 wt % Al_2O_3, (3) 3 wt %

a)Electronic mail: khokim@nongae.gsnu.ac.kr

 0021-8979/97/81(12)/7764/9/$10.00

Al_2O_3, and (4) 5 wt % Al_2O_3. Details of the target preparation are found elsewhere.[17] The density of the sintered targets was $\sim 2.6 \pm 0.2$ g/cm^3.

The sputtering system for AZO film deposition consisted of three target systems equipped with 600 W rf power generators. Corning (7059) glass 0.5 mm thick was used as the substrate. The base pressure in the chamber was $\sim 5 \times 10^{-6}$ Torr and the working pressure (P_w) was controlled in the range from 1 mTorr to 10 mTorr with a high purity Ar gas. The substrate temperature (T_s) was varied from room temperature (RT) to 300 °C, and the rf power(P_{rf}) was varied from 50 W to 300 W. The distance between the target and the substrate was ~ 6 cm. Due to its practical applicability as a transparent conductive film, the ~1500-Å-thick samples were prepared for optical and electrical measurements. Samples for SEM and EDS measurements were prepared on glass substrates with ~ 3 μm thickness due to the probe depth. AZO films ~3000 Å thick were prepared on the Si wafer for RBS analysis. The growth rate and the thickness of the samples were determined by SEM cross-sectional and RBS analyses.

The crystal structure and the crystallinity of the samples were investigated by XRD in θ-2θ geometry. A Ni-filtered Cu K_α($\lambda = 1.5418$ Å) source was used, and the scanning range was between $2\theta = 20$ and 70°. The surface morphology of the films was evaluated by the SEM micrographs. The crystallinity of the samples was observed by SEM cross section. The chemical composition and Al concentration in the films were investigated by EDS and RBS. For RBS analysis, a 2 MeV $^4He^{++}$ ion beam was incident perpendicular to the sample and the backscattered ions were detected at 170°. The RUMP program was used to determine the thickness and the composition of the samples.

The resistivity and Hall coefficient were measured by a Hall automatic measuring system (Bio-Rad Co., UK) using a van der Pauw geometry. Samples were cut ~10 mm ×10 mm square with four Al electrodes, 1 mm radius quarter circles, at each corner for ohmic contact. Transmittance in the visible range was measured by ultraviolet-visible (UV-vis) spectrophotometry. The transmittance was automatically calibrated against a bare glass as a reference sample, and the absorption coefficient was obtained from the transmittance curve.

III. RESULTS AND DISCUSSIONS

A. Structural characterization

The Al content in the sputtering targets and AZO films was investigated by EDS and RBS. In the EDS spectra, peaks at 0.518 keV, 1.109 keV, 8.635 keV, and 9.577 keV are O $K\alpha$, Zn $L\alpha$, Zn $K\alpha$, and Zn $K\beta$, respectively. The peak at 1.496 keV is the Al $K\alpha$ peak. The atomic percent of Al in the targets is 1.8 at. % for the 1 wt % target, 4.2 at. % for the 3 wt % target, and 7.0 at. % for the 5 wt % target, respectively. The Al content in the AZO films prepared with different targets are summarized in Table I. All samples are prepared at $T_s = 150$ °C, $P_{rf} = 150$ W, but at P_w. Even if the detection limit of the quantitative analysis by EDS (~ 0.5 at. %) is considered, the Al content in the films is nearly the same as that in the sputtering target and is independent of the working pressure. Through wavelength dispersive spectrometry (WDS) analysis Igasaki and Saito[19] have also pointed that the amount of Al in the AZO film is nearly the same as the amount of Al_2O_3 in the target and it is almost independent of the deposition parameters.

TABLE I. Al content in the AZO film vs Al_2O_3 content in the sputtering target. AZO films were prepared at $T_s = 150$ °C, $P_{rf} = 150$ W and at different P_w.

Al_2O_3 (wt %)	Al (at. %)		
	P_w = 2 mTorr	P_w = 5 mTorr	P_w = 10 mTorr
1	1.9	2.0	2.0
3	4.0	3.8	3.8
5	6.2	6.0	6.0

Figure 1 shows a representative RBS spectrum for AZO films prepared on the Si substrate at $T_s = 150$ °C, $P_w = 2$ mTorr, and $P_{rf} = 150$ W using a 3 wt % Al_2O_3 target. The yield scale of the backscattered ions is expressed in log-scale in order to show the Al doping effect. By RUMP simulation of the spectrum we found that the AZO film is stoichiometric, i.e., Zn:O is ~1:1 and the Al amount in the film is ~4 at. %, which is again consistent with the EDS measurement.

We investigated how the growth rate is related to the deposition parameters T_s, P_w, and P_{rf}. Figure 2 shows variations of the growth rate with respect to P_{rf}, T_s, and P_w obtained from the samples prepared with a 3 wt % Al_2O_3 target. The growth rate increases with P_{rf} when the samples are prepared at $T_s = 150$ °C and $P_w = 2$ mTorr. This increase indicates that the number of atoms sputtered from the target is proportional to the rf power. The growth rate per unit of rf power is about 1.35 Å/min W at $P_{rf} = 150$ W. As is shown in Fig. 2b, when samples are prepared at $P_{rf} = 150$ W and $P_w = 2$ mTorr, the growth rate decreases and it saturates at T_s higher than 250 °C. The saturation above 250 °C is probably due to the balance between the number of atoms arriving at the substrate surface and the number of atoms

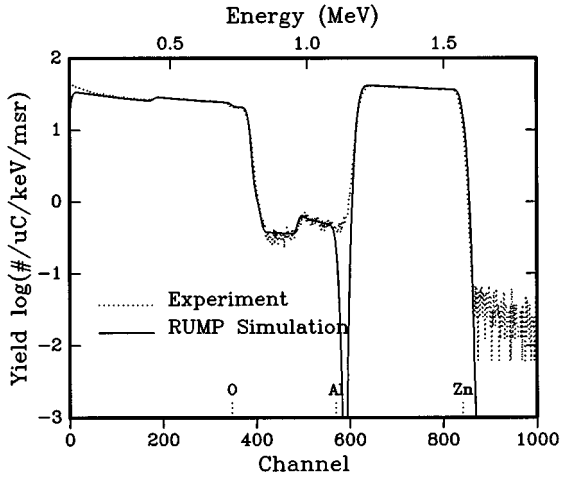

FIG. 1. Representative RBS spectrum of the AZO film. In order to identify the dopant peak (Al) the backscattering yield is plotted in log-scale.

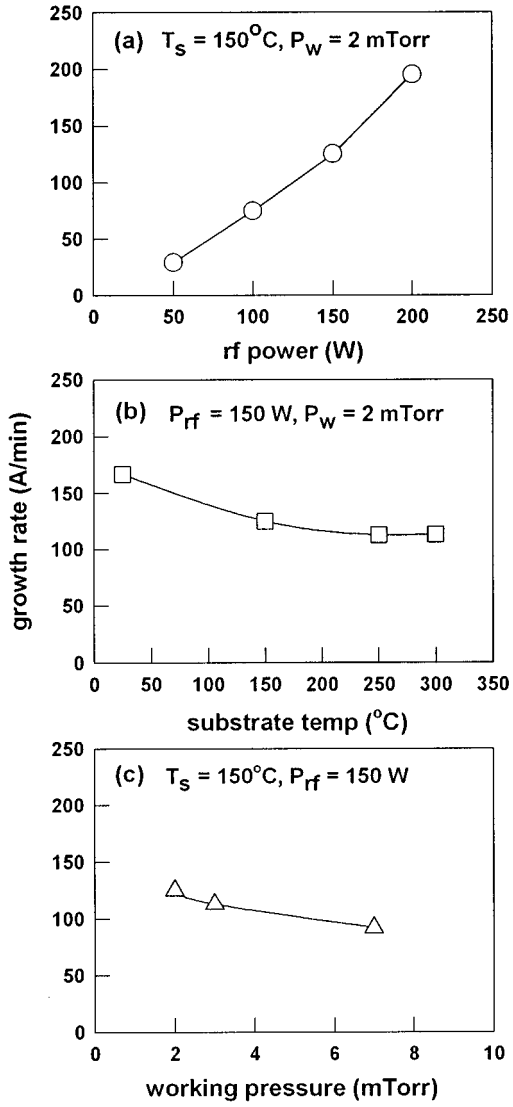

FIG. 2. Growth rate of AZO films as a function of (a) rf power (T_s= 150 °C, P_w=2 mTorr), (b) substrate temperature (rf power = 150 W, P_w=2 mTorr), and (c) working pressure (rf power = 150 W, T_s = 150 °C). T_s and P_w are the substrate temperature and the working pressure, respectively.

bolting out by thermal desorption from the substrate surface, as well as due to the lateral growth by the increase in substrate temperature.[20] Since the surface mobility of an adatom is limited at low substrate temperature, the growth rate becomes larger, but the film has high porosity.[20] Fig. 2c shows the variation of the growth rate with P_w. The growth rate decreases as P_w increases. This is due to the decrease of the mean free path of the sputtered atoms with the increase of P_w.

Figure 3 shows the XRD spectra obtained from ~1500-Å-thick AZO films prepared by different sputtering targets at T_s=150 °C, P_w=2 mTorr, and P_{rf}=150 W. As shown in Fig. 3, only the ZnO(002) peak is observed at 2θ ~34.2° for all samples. This indicates that the AZO films prepared by rf magnetron sputtering show a good *c*-axis orientation that is, the vertical growth to the substrate.[14,15,19] The *c*-axis orientation in AZO films can be understood by

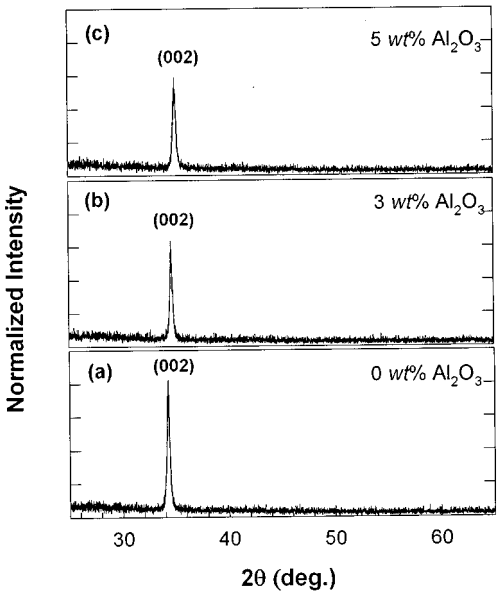

FIG. 3. X-ray diffraction spectra of AZO films prepared on a glass substrate by rf magnetron sputtering with (a) 0, (b) 3 wt %, and (c) 5 wt % Al_2O_3 in the target (rf power = 150 W, T_s=150 °C, and P_w=2 mTorr). The XRD pattern obtained from the ZnO+3 wt % Al_2O_3 target is shown in (d) for comparison.

the ''survival of the fastest'' model proposed by Drift.[18] According to this model, nucleations with various orientations can be formed at the initial stage of the deposition and each nucleus competes to grow but only nuclei having the fastest growth rate can survive, i.e., *c*-axis orientation is achieved. In addition to the *c*-axis orientation a little shift of the peak position of the (002) plane is observed with variation of the Al content in the film. From EDS and RBS analyses the amount of Al in the AZO film prepared by the 3 wt % Al_2O_3 target is ~4.0 at. % and that prepared by the 5 wt % Al_2O_3 target is ~6.2 at. %. Because the ionic radii of Zn^{+2} and Al^{+3} are 72 pm and 53 pm, the lengths of the *c*-axis are expected to shorten about 1.1% and 1.8%, respectively, if all the Al atoms are substituted into Zn sites in the crystal. Thus the position of the ZnO(002) peak is expected to shift ~ 0.4° for the 3 wt % Al_2O_3 target and 0.6° for the 5 wt % Al_2O_3 target to larger 2θ value. Fig. 3 shows a shift in the peak positions of AZO(002) by ~0.4° for the 3 wt % Al_2O_3 target and by ~ 1.0° for the 5 wt % Al_2O_3 target from the pure ZnO film. This indicates that most Al atoms in the AZO films are substituted in the Zn site.

Figure 4 shows the intensity and the full width at half-maximum (FWHM) of the ZnO(002) XRD peak obtained from ~1500-Å-thick AZO films prepared with the 3 wt % Al_2O_3 target. All the samples were prepared at P_w=2 mTorr and P_{rf}=150 W in order to see the effect of substrate temperature on the crystallinity and the grain size. As T_s increases from room temperature to 250 °C, the intensity increases dramatically, but it decreases at 300 °C. The FWHM decreases to 250 °C but increases slightly at 300 °C. The results indicate that the AZO film prepared at 250 °C should have the best crystallinity. According to Thornton's structure zone model,[21] the microstructure of the sputter-deposited metal film depends mainly on P_w, P_{rf}, and T_s.

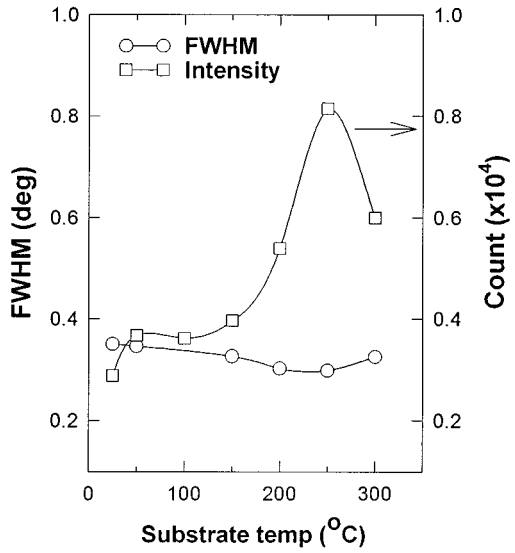

FIG. 4. Variation of AZO(002) peak intensity and FWHM as a function of substrate temperature (rf power=150 W, P_w=2 mTorr).

From the model, the corresponding T_s/T_m (T_m: melting temperature of metal) for columnar growth at P_w between 1 mTorr and 5 mTorr is in the range of 0.25–0.4. If T_m of AZO is the same as that of ZnO (T_m=2250 K), then the T_s for columnar growth is in the range of 290–630 °C. Even though ZnO is highly conductive oxide, it is not a metal. Because its surface is exposed to the high plasma density during rf sputtering, Van der Pol *et al.*[20] pointed out that T_m of ZnO film should be calibrated at ~1400 K. Thus, T_s for the columnar growth region is in the range of 80–290 °C. The results of Fig. 4 indicate that the decrease of the intensity and the increase of the FWHM of the AZO(002) peak prepared at T_s= 300 °C are due to the growth in the transition region where the columnar grains change their grain structure.

We also investigated the intensity and FWHM of the (002) peak of the AZO films prepared at T_s=150 °C and P_{rf}=150 W, but at different P_w. The intensity of the AZO(002) peak at P_w=2 mTorr is the most intense and, as P_w increases, the peak intensity is monotonically decreased to ~70% at 5 mTorr and ~30% at 10 mTorr. This is probably due to the fact that, as P_w increases, the collision probability between the sputtered atoms and Ar ions increases so that the energy of the atoms arriving at the substrate surface is reduced and surface migration is limited. The Ar ions embedded in the film also surface limit surface migration. These factors indicate that the excess working pressure is also one of the impediments to qualified film growth.

Figure 5 shows SEM micrographs of the AZO films prepared using the 3 wt % Al_2O_3 target at P_w=2 mTorr and P_{rf}=150 W. The grain size of the film prepared at room temperature is about 0.1–0.2 μm. The grain size of the AZO films prepared at T_s=150–300 °C is ~0.6 μm. As T_s increases, the grains become densely packed and have a hexagonal shape as shown in the SEM surface micrograph. The grain size can also be deduced from x-ray diffraction by

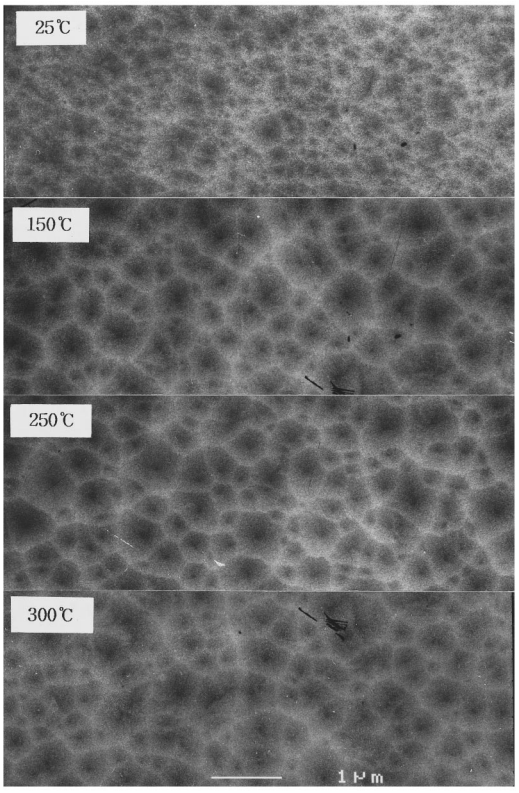

FIG. 5. SEM micrographs of the AZO films prepared on a glass substrate at different substrate temperatures (rf power=150 W, P_w=2 mTorr).

$$t=\frac{0.9\lambda}{\Delta\theta\cos\theta_B}, \tag{1}$$

where t is the grain size, $\Delta\theta$ is the FWHM, and θ_B is the Bragg angle. Using θ_B=17.1°, $\Delta\theta$=0.005°, and λ=1.5418 Å, the grain size t is estimated to be ~330 Å. As shown in SEM surface micrographs, the grain size is ~ 20 times larger than that estimated from the XRD data. This difference is due to the difference in thickness between the SEM samples (~3μm) and the XRD samples (~1500 Å). That is, at the initial stage of film growth, a specified plane grows selectively according to ''survival of the fastest'' model, as the film grows thicker, the larger grain is formed via the aggregation of small grains or grain boundary movement.[22]

Figure 6 shows the cross-sectional SEM micrograph of

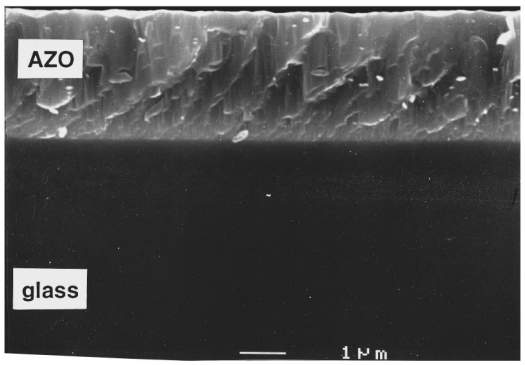

FIG. 6. Cross-sectional SEM micrograph of the AZO film prepared on a glass substrate at T_s= 150 °C (P_{rf}= 150 W, P_w= 2 mTorr).

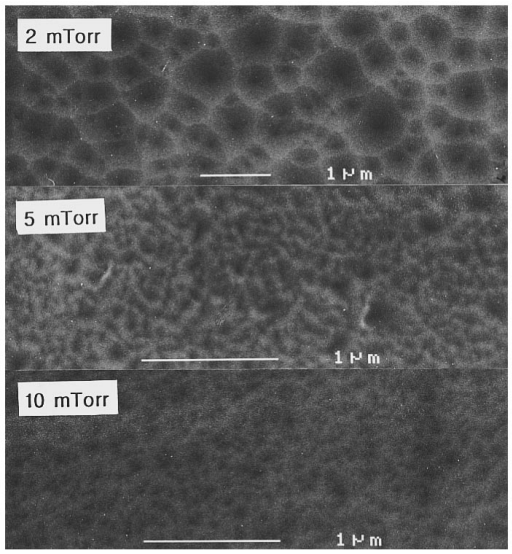

FIG. 7. SEM micrographs of the AZO films prepared at different working pressures. The magnification scales are 15 000×, 20 000×, and 20 000× for samples prepared at 2, 5, and 10 mTorr, respectively (rf power=150 W, T_s=150 °C).

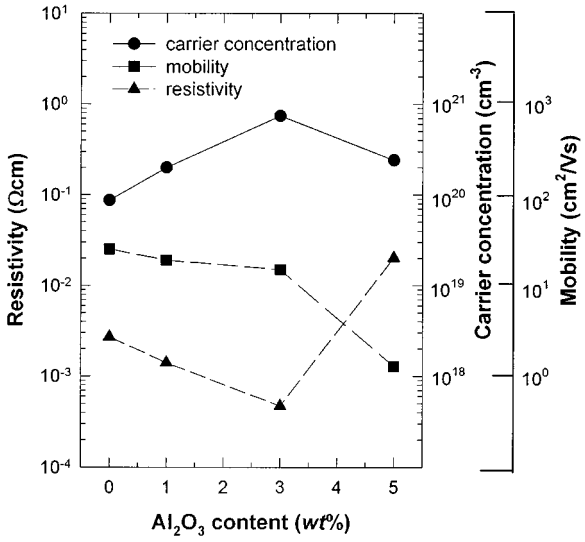

FIG. 8. Plot of the carrier concentration, Hall mobility and resistivity of AZO films as a function of Al_2O_3 content in the target (T_s= 150 °C, rf power= 150 W, P_w= 2 mTorr).

the same sample as that in Fig. 5 (T_s=250 °C). The thickness of the film is ~ 3 μm and the film grows in a columnar structure vertical to the substrate, showing *c*-axis orientation. We obtained the same results as in Fig. 6 for AZO films prepared at different conditions.

Figure 7 shows the SEM surface micrographs of the AZO films prepared at T_s=150 °C and P_{rf}=150 W. As P_w increases, the grain size decreases and the surface roughness increases. This result, in agreement with the XRD analysis, implies that the energy loss from the increase in collision probability of the sputtered atoms and the limitation of surface migration by the adsorbed Ar ions on the film surface lead to rough morphology. Taking into consideration the report by Zin *et al.*[9] on AZO films prepared by reactive cosputtering using Al and ZnO targets at P_w= 5 mTorr having good crystallinity and low resistivity, the optimum working pressure should be reduced when the ZnO target containing Al_2O_3 is used for rf magnetron sputter deposition.

B. Electrical characteristics

The conduction characteristics of ZnO are primarily dominated by electrons generated by the O^{-2} vacancy and Zn interstitial atoms.[23,24] The electrical conductivity in AZO film is higher than that in pure ZnO films due to the contribution from Al^{3+} ions on substitutional sites of Zn^{2+} ions and Al interstitial atoms as well as from oxygen vacancies and Zn interstitial atoms.

Figure 8 shows how the electrical resistivity (ρ), Hall mobility (μ_H), and carrier concentration (n_e) of AZO films are related to the Al_2O_3 content in the sputtering target. All the samples were prepared at the same deposition conditions with T_s=150 °C, P_w=2 mTorr and P_{rf}=150 W. n_e for the pure ZnO film is $\sim 8.7\times 10^{19}/cm^3$, but those for AZO films are more than $10^{20}/cm^3$ regardless of the amount of Al_2O_3 in the target, implying that the deposited AZO films are degenerate semiconductors. As Al_2O_3 in the target increases, n_e also increases and reaches a maximum value of $\sim 7.5\times 10^{20}/cm^3$ for the 3 wt % Al_2O_3 target. On the other hand, n_e decreases to $\sim 2.4\times 10^{20}/cm^3$ for the 5 wt % Al_2O_3 target. EDS and RBS analyses showed that the amounts of Al in the AZO films are 1.9 at. %, 4 at. %, and 6.2 at. % for the 1 wt %, 3 wt %, and 5 wt % Al_2O_3 targets, respectively. The above behavior of n_e suggests that not all the Al atoms in the film contribute to dopants. When impurities are added to ZnO, two kinds of n_e behaviors on dopant concentration are reported. Choi and Im[6] found that, for Ga-doped ZnO film prepared by rf magnetron sputtering using a ZnO + Ga_2O_3 target, excess Ga atoms above a certain critical concentration in the ZnO films are segregated into the grain boundaries. The segregated Ga atoms do not activate as dopants, thus n_e is limited. Minami *et al.*[25,26] reported that, when ZnO film is doped with Al or Si prepared by sputtering using $ZnO+Al_2O_3$ or $ZnO+SiO_2$ targets, n_e increases with increasing amounts of Al_2O_3 or SiO_2, and decreases when the amount of Al_2O_3 or SiO_2 in the target is over ~ 4 wt %. As shown in Fig. 8, the decrease of n_e in AZO film prepared using the 5 wt % Al_2O_3 target suggests that the excess Al atoms do not activate due to segregation at the grain boundary. μ_H decreases from ~ 25.3 $cm^2/V\,s$ for pure ZnO to ~ 1.3 $cm^2/V\,s$ as the amount of Al_2O_3 in the target is increased to 5 wt %. The decrease of μ_H is due to the scattering from the grain boundaries and ionized impurities. μ_H is expressed as,[8]

$$\frac{1}{\mu_H}=\frac{1}{\mu_i}+\frac{1}{\mu_g}, \tag{2}$$

where μ_i and μ_g are mobilities due to impurity scattering and grain boundary scattering, respectively. The gradual decrease of μ_H as the amount of Al_2O_3 is increased to 3 wt % can be understood by the fact that μ_H is dominated by ionized impurity scattering. But the rapid decrease of μ_H in the

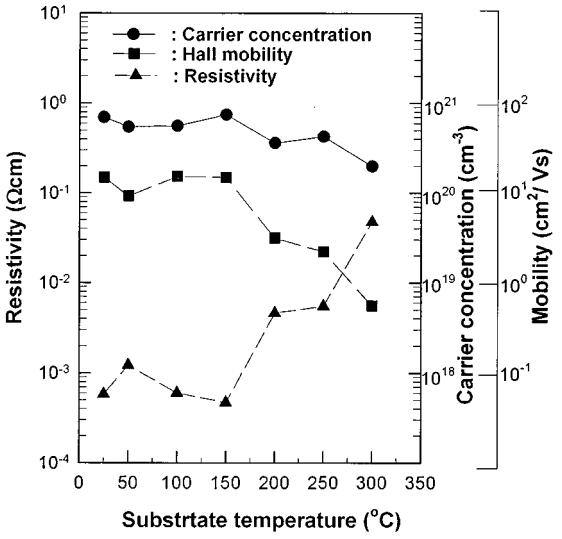

FIG. 9. Plot of the carrier concentration, Hall mobility, and resistivity of AZO films prepared with the 3 wt % Al_2O_3 target as a function of substrate temperature (rf power=150 W, P_w= 2 mTorr).

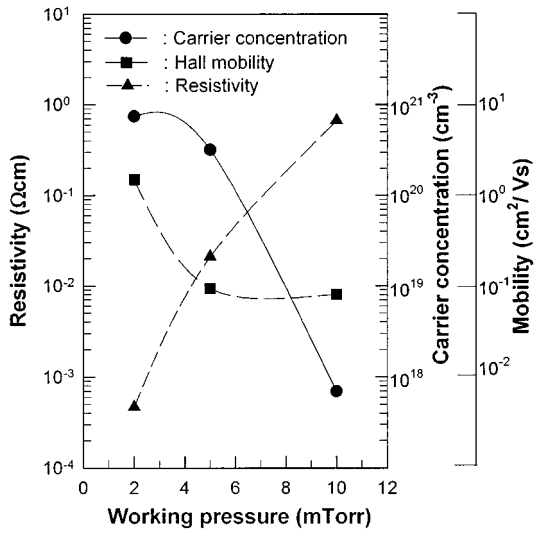

FIG. 10. Plot of the carrier concentration, Hall mobility, and resistivity of AZO films prepared with the 3 wt % Al_2O_3 target as a function of working pressure (rf power= 150 W, T_s=150 °C).

case of the 5 wt % Al_2O_3 target is mainly due to increased grain boundary scattering. ρ decreases from 2.7×10^{-3} Ω cm for pure ZnO film to a minimum value of 4.7×10^{-4} Ω cm for AZO film prepared with the 3 wt % Al_2O_3 target. However ρ increases to 2×10^{-2} Ω cm for AZO film prepared with the 5 wt % Al_2O_3 target. The resistivity of the AZO film is related to the Al-doping concentration, O vacancies, Al and Zn concentrations at interstitial sites, grain boundaries, and ionized impurity scattering.[19] The rapid increase of ρ in the AZO film prepared with the 5 wt % Al_2O_3 target is probably due to both the decrease of n_e and μ_H by the increased grain boundary barrier.

Figure 9 shows the variations of ρ, μ_H, and n_e in the AZO films with respect to T_s. All the samples were prepared with the 3 wt % Al_2O_3 target at P_w= 2 mTorr and P_{rf}= 150 W. In the temperature range from RT to 150 °C, n_e is nearly constant. Above 250 °C, n_e decreases slightly, but is still over 10^{20}/cm^3. μ_H is also nearly constant at temperatures below 150 °C, but decreases rapidly above 200 °C(from 15 cm^2/V s at 150 °C to 0.5 cm^2/V s at 300 °C). ρ is nearly constant below 150 °C and increases rapidly over 200 °C. The AZO film with the highest conductivity is obtained at T_s=150 °C. This (T_s=150 °C) is lower than the 200 °C that was reported by other studies.[6,23,27] The resistivity of the AZO film prepared at T_s=300 °C is $\sim 5 \times 10^{-2}$ Ω cm, which is two orders of magnitude higher than that of the sample prepared at 150 °C. The RBS results showed that the O/Zn ratio in the AZO film prepared at 50 °C, 100 °C, and over 150 °C was 0.95, 0.98 and 0.99, respectively. This is an indication that the O vacancies in AZO films play an important role for conduction in AZO films. From the XRD results for samples prepared at various T_s with the 3 wt % Al_2O_3 target, the minimum value of the FWHM and the maximum value of the diffraction intensity of the (002) peak were obtained from the sample prepared at 250 °C. The SEM surface micrographs (Fig. 5) also show that the grain boundary width of films prepared at higher T_s increases, and this implies that the potential barrier at grain boundaries has increased greatly. Thus the increase of ρ and the decrease of μ_H in the AZO films prepared at higher T_s are ascribed to the increased grain boundary barrier.

Figure 10 shows the Ar working pressure dependence of ρ, μ_H, and n_e of AZO films prepared with the 3 wt % Al_2O_3 target at T_s=150 °C and P_{rf}=150 W. As P_w increases, n_e and μ_H decrease. Notice that ρ increases by ~3 times more from 4.7×10^{-4} Ω cm at 2 mTorr to 0.8 Ω cm at 10 mTorr. The increase of ρ is due to the decrease of n_e and μ_H in the samples prepared at higher P_w. As can be seen from the SEM surface micrographs (Fig. 7), the grain size in the films prepared at 5 mTorr and 10 mTorr decreases to 1/10 and 1/15, respectively, compared to that prepared at 2 mTorr, and the porosity of the films also increases greatly. Because the AZO films are chemically very active, the chemisorbed O atoms at the film surface absorb electrons from the conduction band. This leads to the decrease of n_e, and widening of the depletion layer.[19] The decrease of μ_H is largely due to the increase of the grain boundary barrier height by poor crystallinity.

In order to clarify that the conductivity is directly related to the crystallinity of the AZO films, we plotted the resistivity versus FWHM of the ZnO(002) diffraction peak in Fig. 11. As the FWHM decreases, the resistivity decreases. This is an indication that the conductivity is strongly dependent on the crystallinity of the AZO film. The electrical transport properties of the AZO films are dominated by either n_e or μ_H. Figure 12 shows how the resistivity is related to the carrier concentration and Hall mobility. As is shown in Fig. 12, ρ is more closely related to μ_H than to n_e. Minami *et al.*[26,27] also found that the low resistivity ($\sim 2.7 \times 10^{-4}$ Ω cm) of the AZO films prepared by rf magnetron sputtering is due to the high Hall mobility.

In this experiment, the minimum value of ρ of 4.7×10^{-4} Ω cm is obtained from the AZO films prepared with

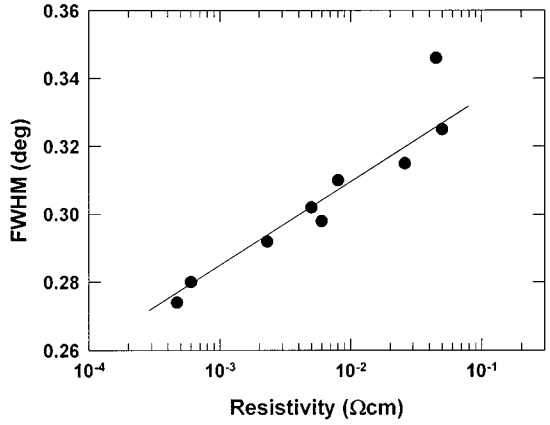

FIG. 11. Plot of the resistivity vs FWHM of the ZnO(002) diffraction peak.

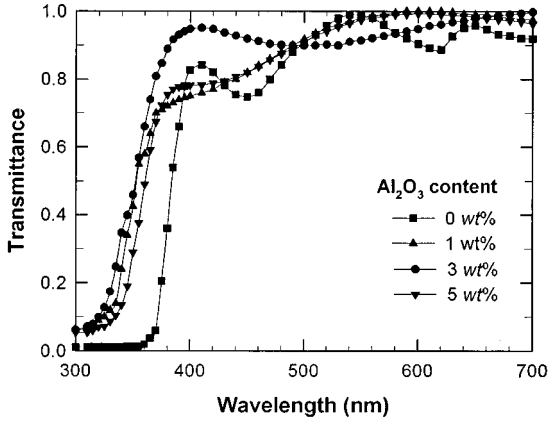

FIG. 13. Optical transmission of AZO films prepared by different amounts of Al_2O_3 in the target (T_s=150 °C, rf power=150 W, P_w= 2 mTorr).

the 3 wt % Al_2O_3 target at T_s=150 °C, P_{rf}=150 W, and P_w=2 mTorr. In this case n_e and μ_H are at a maximum. This indicates that, in order to get highly conducting AZO films by rf magnetron sputtering, it is necessary to optimize growth conditions such as substrate temperature, working pressure, and rf power.

C. Optical characteristics

Figure 13 shows the optical transmittance of ~ 1500-Å-thick AZO films prepared with targets having different Al_2O_3 contents at T_s=150 °C, P_w=2 mTorr and P_{rf}=150 W. The optical transmittance at 550 nm is more than 90% for all samples regardless of the Al_2O_3 content in the target. In the transmittance spectrum for the undoped ZnO film, two absorption peaks at 450 eV and 610 eV are observed. The absorption peak at 610 eV is also found in other experiments,[9,13] and is probably the result of unintentional doping by impurities during film growth. As the Al_2O_3 content increases, the absorption edge shifts monotonically to the shorter wavelength region. However, the absorption edge of the AZO film prepared with the 5 wt % Al_2O_3 target shifts less than that of the 1 wt % sample. The movement of the absorption edge to the shorter wavelength region is the Burstein-Moss shift,[9,10,12,28,29] which is due to the increase of n_e. As shown in Fig. 8, n_e of AZO films increases as the Al_2O_3 amount in the target is increased to 3 wt %, whereas n_e decreases when the Al_2O_3 content is 5 wt %. Thus the shift of the optical absorption edge to shorter wavelength is strongly correlated with n_e. The optical absorption coefficient, α, is defined as

$$I=I_0e^{-\alpha t}, \tag{3}$$

where I is the intensity of transmitted light, I_0 is the intensity of incident light, and t is the thickness of the AZO film (here, 1500 Å). Since the transmittance is defined as I/I_0, we obtain α from Eq. (3). In the direct transition semiconductor, α and the optical energy band gap (E_g) are related by,[30]

$$\alpha=(h\nu-E_g)^{1/2}, \tag{4}$$

where h is Planck's constant, and ν is the frequency of the incident photon. Figure 14 is the plot of α^2 vs $h\nu$. The linear dependence of α^2 to $h\nu$ indicates that AZO films are direct transition type semiconductors. The photon energy at the point where α^2 is zero is E_g. Then E_g is determined by the extrapolation method. From Fig. 14, E_g for the pure ZnO film is ~ 3.3 eV, and the E_g's for samples prepared with the 1 wt %, 3 wt %, and 5 wt % Al_2O_3 targets are ~3.52 eV, 3.54 eV, and 3.47 eV, respectively. The decrease of E_g for the sample prepared with the 5 wt % Al_2O_3 target is in accord with the decrease of n_e.

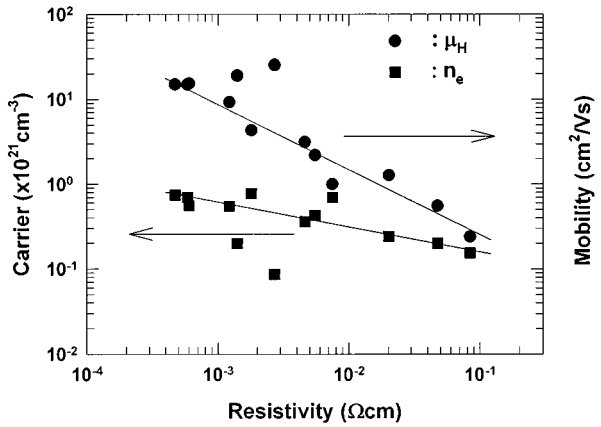

FIG. 12. Plot of the carrier concentration vs resistivity, and the Hall mobility vs resistivity of the AZO films.

Figure 15 shows the relation between α^2 and $h\nu$ for the AZO films prepared at different T_s. All the samples were prepared with the 3 wt % Al_2O_3 target at P_w= 2 mTorr and P_{rf}=150 W. The transmittance is more than 90% at 550 nm for all samples. The E_g's for samples prepared at $T_s \leqslant 200$ °C is 3.53 eV, whereas E_g's for samples prepared at T_s=250 °C and T_s=300 °C are 3.50 and 3.46 eV, respectively. These results are again consistent with the results obtained from Fig. 10.

Burstein[31] pointed out that the increase of the Fermi level in the conduction band of the degenerate semiconductor leads to the energy band widening (blue shift) effect. The energy band gap widening (ΔE_g) is related to n_e through the following equation,

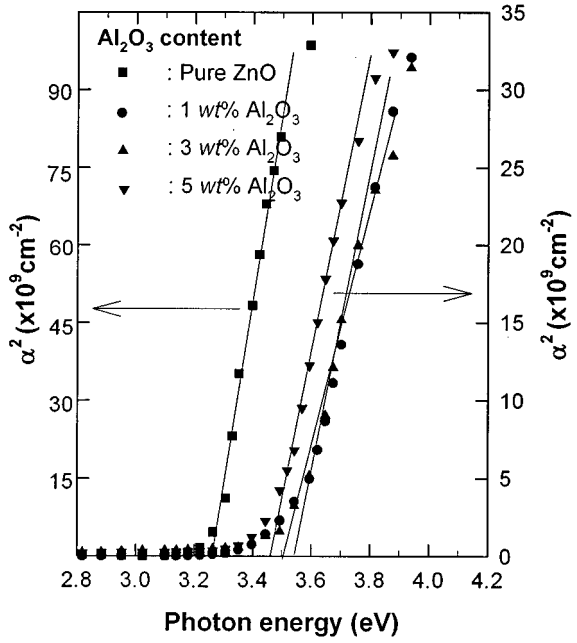

FIG. 14. Square of the absorption coefficient as a function of photon energy for the samples in Fig. 10.

$$\Delta E_g = \frac{h^2}{8m^*}\left(\frac{3}{\pi}\right)^{2/3} n_e^{2/3}, \tag{5}$$

where h is Planck's constant and m^* is the electron effective mass in conduction band. Figure 16 shows the blueshift of the AZO films (the difference of the energy band gap between AZO and pure ZnO film) versus the carrier concentration n_e. The blueshift is proportional to n_e, but does not accurately follow Eq. (5). The exponent in Eq. (5) is 2/3 but

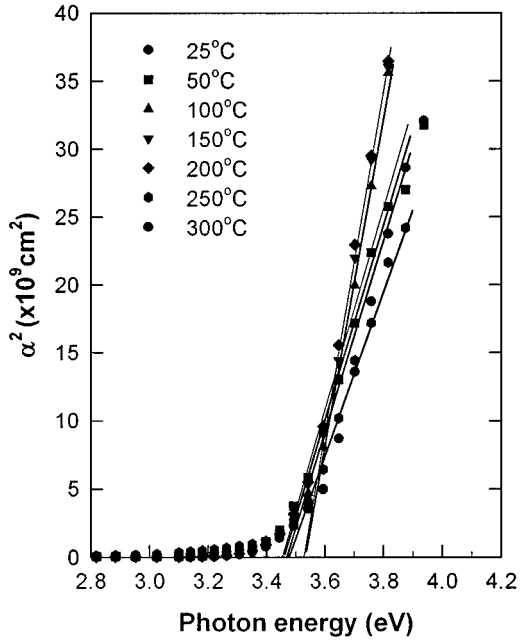

FIG. 15. Square of the absorption coefficient as a function of photon energy for samples prepared at different substrate temperatures using the 3 wt % Al_2O_3 target (rf power=150 W, P_w=2 mTorr).

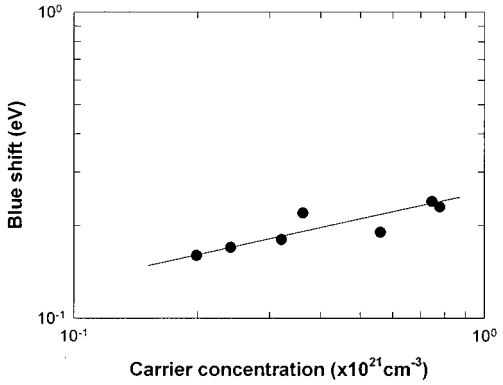

FIG. 16. Dependence of optical energy band gap widening on the carrier concentration.

the experimental value is ~1/3. Choi and Im[6] reported that the exponent is ~3/5 from their Burstein-Moss shift measurements of their Ga-doped ZnO films. Other experiments[10,32] also showed that the exponent is in the range from 1/3 to 2/3. In a high carrier concentration above Mott's critical concentration or in highly excited semiconductors, the electronic state of the materials can be calibrated by electron-electron or electron-impurity scattering. That is, the many-body effect such as exchange interaction or Coulomb interaction makes the energy band gap decrease. Wolff[33] explained that when such a phenomenon is in competition with Burstein-Moss shift for a semiconductor of $n_e \sim 10^{20}/\text{cm}^2$ the exponent obtained from experimental value is not exactly equal to that in Eq. (5).

IV. SUMMARY

Al-doped ZnO (AZO) films were prepared by rf magnetron sputtering with the ZnO target containing different amounts of Al_2O_3. The amounts of Al in the AZO films deduced from EDS and RBS measurements are proportional to the Al_2O_3 amount in the target. The crystal structure of as-prepared AZO films is hexagonal wurtzite and the films are highly oriented along the c-axis, i.e., the AZO(002) plane grows parallel to the substrate. The growth rate increases with increasing P_{rf}, but decreases with increasing T_s and P_w. The intensity of the AZO(002) diffraction peak increases as T_s increases to 250 °C, and it decreases at T_s =300 °C. As P_w increases from 2 mTorr to 5 mTorr, the peak intensities decrease rapidly, indicating that the high Ar pressure limits the growth of AZO films.

Samples with the lowest resistivity, $4.7\times10^{-4}\Omega$ cm, and transmittance over 90% at the visible region were prepared by using the 3 wt % Al_2O_3 target at T_s= 150 °C, P_w=2 mTorr, and P_{rf}=150 W. n_e increases from ~ $8.7\times10^{19}/\text{cm}^3$ for undoped ZnO to ~$7.5\times10^{20}/\text{cm}^3$ for the AZO film prepared with the 3 wt % Al_2O_3 target, but decreases to ~ $2.4\times10^{20}/\text{cm}^3$ for sample prepared with the 5 wt % Al_2O_3 target. This indicates that not all Al atoms in the film are activated. μ_H is dominated mostly by grain boundary scattering rather than by ionized impurity scattering.

AZO films are degenerate semiconductors with a direct optical energy band gap. The optical energy band gap for

undoped ZnO film is ~3.3 eV and that those for AZO films increases as n_e in the target increases. The blueshift in the AZO films is proportional to a one-third power of n_e.

ACKNOWLEDGMENTS

The authors would like to acknowledge to Professor M.-A. Nicolet for helpful discussions and RBS measurements at Caltech. This work was supported in part by the Ministry of Education, Korea, under Contract No. BSRI-96-2406, the Korea Science and Engineering Foundation (KOSEF) under Contract No. 951-0204-047-2, and by the Sensor Technology Research Center under Contract No. 95K4-0602-17-1.

[1] C. G. Granqvist, Thin Solid Films **193/194**, 730 (1990).
[2] K. Vanheusden, W. L. Warren, C. H. Seager, D. R. Tallant, J. A. Voight, and B. E. Gnade, J. Appl. Phys. **79**, 7983 (1996).
[3] K. L. Chopra, S. Major, and D. K. Pandya, Thin Solid Films **102**, 1 (1983).
[4] K. H. Kim and T. S. Park, J. Korean Phys. Soc. **18**, 124 (1985).
[5] T. Minami, H. Sato, H. Nanto, and S. Takata, Jpn. J. Appl. Phys. 1 **125**, L776 (1986).
[6] B. H. Choi and H. B. Im, Thin Solid Films **193/194**, 712 (1990).
[7] G. A. Hirata, J. McKittrik, T. Cheeks, J. M. Siqueiros, J. A. Diaz, O. Contreras, and O. A. Lopez, Thin Solid Films **288**, 29 (1996).
[8] S. Ghosh, A. Sarkar, S. Chaudhuri, and A. K. Pal, Thin Solid Films **205**, 64 (1991).
[9] Z. C. Zin, I. Hamberg, and C. G. Granqvist, J. Appl. Phys. **64**, 5117 (1988).
[10] B. E. Selnelius, K. F. Berggren, Z. C. Zin, I. Hamberg, and C. G. Granqvist, Phys. Rev. B **37**, 10 244 (1988).
[11] S. Takata, T. Minami, and H. Nanto, Thin Solid Films **135**, 183 (1986).
[12] T. Minami, H. Nanto, and S. Takata, Jpn. J. Appl. Phys. 1 **124**, L605 (1985).
[13] T. Minami, H. Nanto, and S. Takata, Jpn. J. Appl. Phys. 1 **23**, L280 (1984).
[14] K. Tominaga, M. Kataoka, H. Manabe, T. Ueda, and I. Mori, Thin Solid Films **290–291**, 84 (1996).
[15] S. Takada, J. Appl. Phys. **73**, 4739 (1993).
[16] H. C. Weller, R. H. Mauch, and G. H. Bauer, Sol. Energy Mater. Sol. Cells **27**, 217 (1992).
[17] K. C. Park, H. K. Lee, T. Y. Ma, and K. H. Kim, Korean Appl. Phys. **9**, 450 (1996).
[18] A. Van der Drift, Philips Res. Rep. **22**, 267 (1967).
[19] Y. Igasaki and H. Saito, J. Appl. Phys. **70**, 3613 (1991).
[20] F. C. M. Van de Pol, F. R. Blom, and Th. J. A. Popma, Thin Solid Films **204**, 349 (1985).
[21] J. A. Thornton, J. Vac. Sci. Technol. **11**, 666 (1974).
[22] J. C. Lodder, T. Wielinga, and J. Worst, Thin Solid Films **101**, 61 (1983).
[23] Y. Igasaki and H. Saito, J. Appl. Phys. **69**, 2190 (1991).
[24] F. R. Blom, F. C. M. Van de Pol, G. Bauhuis, and Th. J. A. Popma, Thin Solid Films **204**, 365 (1991).
[25] T. Minami, S. Sato, H. Nanto, and S. Takata, Jpn. J. Appl. Phys. 1 **24**, L781 (1985).
[26] T. Minami, H. Nanto, and S. Takata, Jpn. J. Appl. Phys. 1 **25**, L776 (1986).
[27] T. Minami, K. Oohashi, and T. Sakata, Thin Solid Films **193–194**, 721 (1990).
[28] B. E. Sernelius, Phys. Rev. B **36**, 4878 (1987).
[29] I. Hamberg, C. G. Granqvist, K. F. Berggren, B. E. Sernelius, and L. Engstron, Phys. Rev. B **30**, 3240 (1984).
[30] E. Ziegler, A. Heinrich, H. Oppermann, and G. Stover, Phys. Status Solidi A **66**, 635 (1981).
[31] E. Burstein, Phys. Rev. **25**, 7826 (1982).
[32] A. P. Roth, J. B. Webb, and D. F. Williams, Phys. Rev. B **25**, 7826 (1982).
[33] P. A. Wolff, Phys. Rev. **126**, 405 (1962).